JOURNAL OF VIROLOGY, Apr. 1997, p. 2959–2969 Vol. 71, No. 4
0022-538X/97/$04.00+0

Evolution of Mouse Hepatitis Virus: Detection and Characterization of Spike Deletion Variants during Persistent Infection

CYNTHIA L. ROWE,[1] SUSAN C. BAKER,[1] MEERA J. NATHAN,[2] AND JOHN O. FLEMING[2]*

Department of Microbiology and Immunology and Molecular Biology Program, Loyola University of Chicago, Stritch School of Medicine, Maywood, Illinois 60153,[1] and Departments of Neurology and Medical Microbiology, University of Wisconsin and William S. Middleton Veterans Hospital, Madison, Wisconsin 53792[2]

Received 30 September 1996/Accepted 13 December 1996

High-frequency RNA recombination has been proposed as an important mechanism for generating viral deletion variants of murine coronavirus. Indeed, a number of variants with deletions in the spike glycoprotein have been isolated from persistently infected animals. However, the significance of generating and potentially accumulating deletion variants in the persisting viral RNA population is unclear. To study this issue, we evaluated the evolution of spike variants by examining the population of spike RNA sequences detected in the brains and spinal cords of mice inoculated with coronavirus and sacrificed at 4, 42, or 100 days postinoculation. We focused on the S1 hypervariable region since previous investigators had shown that this region is subject to recombination and deletion. RNA isolated from the brains or spinal cords of infected mice was rescued by reverse transcription-PCR, and the amplified products were cloned and used in differential colony hybridizations to identify individual isolates with deletions. We found that 11 of 20 persistently infected mice harbored spike deletion variants (SDVs), indicating that deletions are common but not required for persistent infection. To determine if a specific type of SDV accumulated during persistence, we sequenced 106 of the deletion isolates. We identified 23 distinct patterns of SDVs, including 5 double-deletion variants. Furthermore, we found that each mouse harbored distinct variants in its central nervous system (CNS), suggesting that SDVs are generated during viral replication in the CNS. Interestingly, mice with the most severe and persisting neurological disease harbored the most prevalent and diverse quasispecies of SDVs. Overall, these findings illustrate the complexity of the population of persisting viral RNAs which may contribute to chronic disease.

The murine coronavirus mouse hepatitis virus JHM (MHV-JHM) causes acute and chronic neurological disease upon infection of the central nervous system (CNS) of susceptible rodents and has been intensively studied as an experimental model of human demyelinating diseases such as multiple sclerosis (10, 16, 34). The type of disease induced by MHV-JHM depends on the strain of virus, the age and type of animal, the amount of virus and route of inoculation, the host immune status, and other experimental variables. Infection of mice with attenuated strains of MHV-JHM often causes robust subacute and chronic demyelination (11, 17, 18, 31, 40, 49, 54, 55). For example, recent studies with MHV-JHM 2.2-V-1 have shown that mice have prolonged paralysis and that persisting viral RNA can be rescued from the CNS of these animals by reverse transcription (RT)-PCR for up to 787 days postinoculation (p.i.) (21) whereas infectious virus is typically cleared by 15 to 20 days p.i. Because of possible parallels of this experimental model with chronic CNS diseases of humans and animals, we sought to study the nature of the viral RNA that persists during chronic MHV-JHM 2.2-V-1 infection and to examine its role in pathogenesis.

MHV-JHM is an enveloped virus with a 32-kb single-stranded RNA genome of positive polarity (24, 48). The MHV virion is composed of four structural proteins: spike (S), membrane (M), small membrane (sM), and nucleocapsid (N). In addition, some strains of MHV express the hemagglutinin-esterase (HE) glycoprotein. The spike glycoprotein (180 kDa) is proteolytically processed to two 90-kDa subunits, termed S1 and S2 (50). The spike glycoprotein is critical for receptor binding and fusion with susceptible cells and is the target of neutralizing antibodies (8). Studies with monoclonal antibodies (MAbs) directed against the spike found that viruses which escape neutralization were neuroattenuated, suggesting that the spike plays a major role in MHV pathogenesis (11, 17, 55). Furthermore, these MAb escape variants were shown to have deletions in the "hypervariable" region of S1 (nucleotides [nt] 1200 to 1800), implicating this region as a major determinant for MHV neurovirulence (2, 43, 52, 53).

Many investigators have shown that during persistence of MHV in vivo, variants with deletions in the S gene are produced (see Fig. 1). Often, such variants have shown interesting pathogenic properties such as reduced neurovirulence or increased tropism for white matter. Also, genetic studies have shown that the deletions in the S gene tend to cluster in a hypervariable region near the same region deleted in MAb escape mutants. The nature and significance of deletions in the S gene remain unclear. One limitation of previous studies is that they have focused exclusively on variants which produce infectious virus. It is possible that these variants represent a selected subpopulation of persisting genomes. Furthermore, such variants have generally been isolated subacutely, at the time that infectious virus is waning. Therefore, we sought to characterize the population of viral RNA which persists at later time points, when disease is chronic and infectious virus typically cannot be recovered.

To address these issues, we developed a system to analyze the population of persisting MHV RNA species and to identify

* Corresponding author. Phone: (608) 263-5421. Fax: (608) 263-0412. E-mail: fleming@neurology.wisc.edu.

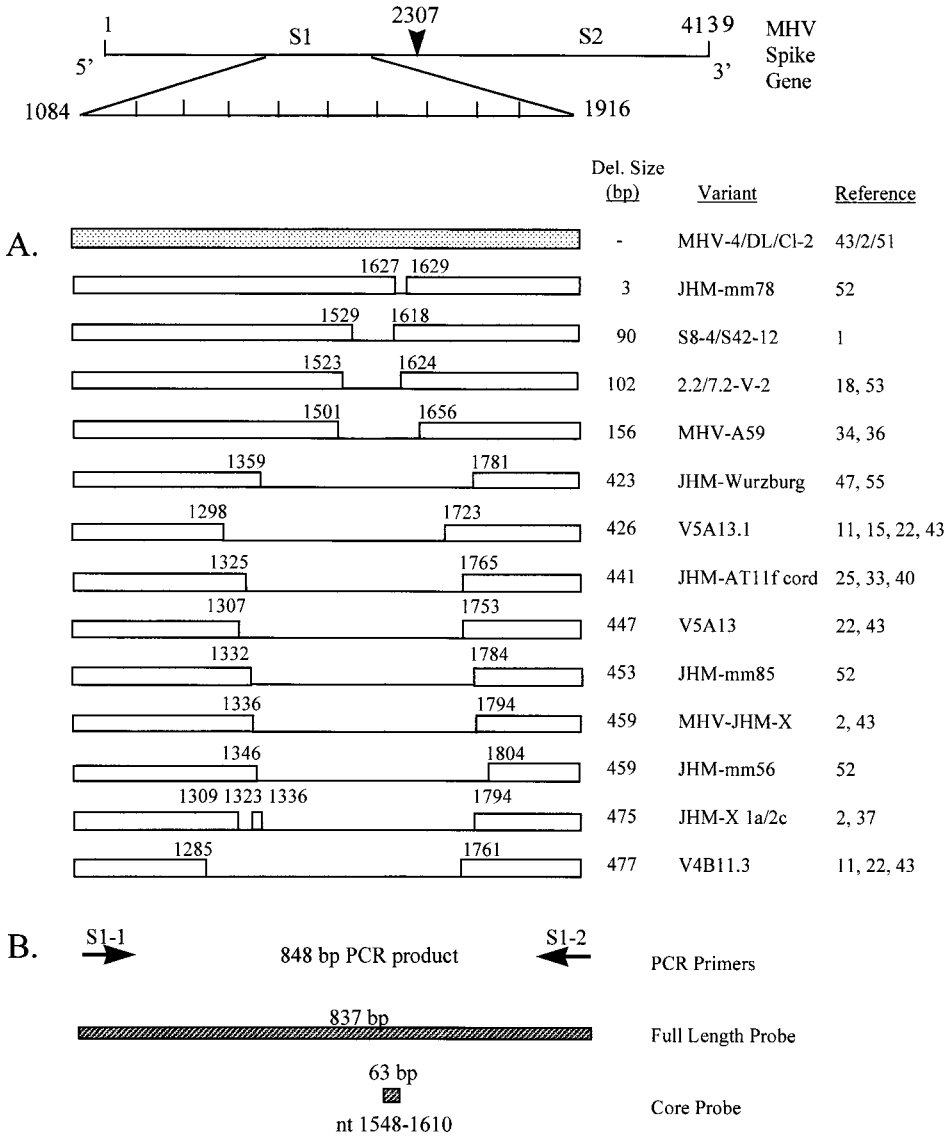

FIG. 1. (A) Schematic representation of the 4,139-nt MHV-JHM spike gene sequence and previously identified variants containing deletions in the 3′ region of S1. Nucleotide designations represent the first and last positions of the deleted region (i.e., 1627 to 1629 indicates that nt 1627, 1628 and 1629 are deleted). For ambiguous cases, the deletion was defined as the 5′-most deletion possible. (B) Location of the PCR primer pair used to amplify S1 cDNA from the brains and spinal cords of mice inoculated with MHV-JHM and of the full-length and core probes (837 and 63 bp, respectively) used in differential colony hybridization to identify individual transformants containing S1 deletions.

and characterize the MHV spike deletion variants (SDVs) in the population. We rescued the S1 region of the spike RNA, known to be hypervariable, from the brains and spinal cords of experimental mice by RT-PCR. This technique allowed us to examine the population of persisting coronavirus RNA species without bias or requirement that they generate infectious virions. We systematically studied the prevalence and nature of deletions in the S1 region by cloning, differential hybridization, and sequencing individual isolates. We show that SDVs are common but are not required for persistent infection. When SDVs were present during persistent infection, each mouse harbored distinct variants in their CNS, suggesting that SDVs are generated de novo and not from amplification of preexisting variants in the input pool. With regard to biological significance, we found that SDVs were most prevalent in the spinal cord RNA of mice with the most severe and prolonged neurological impairment, suggesting an important role for SDVs as a consequence or cause of disease during MHV persistence in the CNS.

MATERIALS AND METHODS

Virus. MHV-JHM 2.2-V-1, a neuroattenuated variant of JHM-DL, was propagated in DBT cells and assayed as previously described (17). MHV-JHM 2.2-V-1 causes predominantly subacute and chronic demyelination in mice (17). The entire spike gene of 2.2-V-1 has been sequenced and differs from the parental strain JHM-DL spike gene sequence at one nucleotide (nt 3340) in the S2 region of the spike gene, which results in an amino acid change from leucine to phenylalanine (53).

Mice. Six-week-old male C57BL/6J mice (Jackson Laboratories, Bar Harbor, Maine) were used in these experiments. Upon arrival, selected mice were tested and found to be seronegative for murine coronavirus by enzyme-linked immunosorbent assay (19). The mice were inoculated intracerebrally with 10^3 PFU of MHV-JHM 2.2-V-1 (17) and periodically monitored for signs of paralytic disease on a scale of 0 (normal) to 4 (paraplegia) (20). The mice were sacrificed by CO_2

inhalation on days 4, 42 and 100 p.i. The brains and spinal cords were removed aseptically, immediately frozen on dry ice, and stored at −70°C.

RNA extraction. Brains and spinal cords were thawed, and each half brain and spinal cord was manually disrupted in a Tenbrock homogenizer containing 4 ml (brain) or 2 ml (cord) of RNA STAT (Tel-test Inc., Friendswood, Tex.) and incubated for 5 min at room temperature. RNA was subsequently extracted by addition of 0.2 ml of chloroform/ml of RNA STAT. The phases were separated by centrifugation at 13,800 × *g* for 15 min at 4°C. The aqueous phase was removed, and the RNA was precipitated in the presence of 0.5 ml of isopropanol at room temperature for 10 min. The RNA was pelleted by centrifugation for 10 min at 13,800 × *g* and 4°C, and the pellet was washed with 1 ml of 75% ethanol and then air dried for 5 to 6 min. Brain RNA pellets were resuspended in 25 μl of diethylpyrocarbonate-treated water, and spinal cord RNA pellets were resuspended in 20 μl of diethylpyrocarbonate-treated water. The RNA quantity was determined by optical density measurements at 260 nm. The integrity of the total RNA was assessed by RT-PCR for β_2-microglobulin mRNA. Input virus RNA was isolated by mixing 5×10^6 PFU of MHV-JHM 2.2-V-1 with half of an uninfected mouse brain and immediately subjecting the mixture to RNA extraction as described above.

RT-PCR of brain and spinal cord RNAs. Brain or spinal cord RNA (2 μg per sample) was denatured with 20 mM methyl mercury hydroxide for 5 min at room temperature, and β-mercaptoethanol was added at a final concentration of 0.14 M. For cDNA synthesis, the RNA was incubated at 42°C for 60 min in a reaction mixture containing 50 mM Tris-HCl (pH 8.3), 50 mM KCl, 10 mM $MgCl_2$, 10 mM dithiothreitol, 0.5 mM spermidine, 1.25 mM of each deoxynucleoside triphosphate, 40 U of RNasin, 1 μg of random hexamer oligonucleotide primers, and 12.5 U of avian myeloblastosis virus reverse transcriptase (Promega, Madison, Wis.). (The RT reaction mixture was preincubated for 30 min on ice prior to cDNA synthesis.) The cDNA synthesis reaction was overlaid with a wax plug (PCR Gems; Perkin-Elmer Cetus, Branchburg, N.J.) and then heat inactivated at 95°C for 3 min and quickly cooled on ice.

The synthesized cDNA was amplified by PCR, using a method adapted from that of Saiki et al. (44) and Chang et al. (7) to minimize errors introduced by *Taq* polymerase. Briefly, 20 μl of RT mixture was mixed with 80 μl of a master mix buffer containing 7.5 mM Tris-HCl (pH 9.0), 0.075% Triton X-100, 0.25 μM synthetic oligonucleotide primers S1-1 and S1-2 (1), and 2.5 U of *Taq* polymerase (Promega). The PCR mixture was laid over the wax plug and subjected to 40 cycles of amplification, with each cycle consisting of 94°C for 1 min, 60°C for 1 min, and 72°C for 1 min. At the end of this period, an additional extension step at 72°C for 7 min was performed. RT-PCR products were purified by the Wizard PCR Preps DNA purification system (Promega), and 1/10 of the reaction products were analyzed by electrophoresis on a 1.5% agarose gel for 1 h at 100 V in 1× TBE (Tris-borate-EDTA) and visualized by ethidium bromide staining.

Cloning RT-PCR products. Purified RT-PCR products were ligated into the cloning vector pGEM-T (Promega). RT-PCR products which were not initially detected by analysis of 1/10 of the reaction products by ethidium bromide staining of a 1.5% agarose gel were concentrated by precipitation with 1 μl of glycogen–1/10 volume of 5 M ammonium acetate–2.5 volumes of 100% ethanol prior to ligation. The ligation reaction mixture included 30 to 50 ng of the RT-PCR products, 1 U of T4 DNA ligase (Gibco-BRL), 50 ng of pGEM-T, 50 mM Tris-HCl (pH 7.6), 10 mM $MgCl_2$, 1 mM ATP, and 1 mM dithiothreitol, and the reaction was carried out at 14°C overnight. The ligation reactions were used to transform high-efficiency competent *Escherichia coli* DH5α cells (Bethesda Research Laboratories). Blue/white selection was used to identify insert-containing colonies, which were picked and stabbed in duplicate in a grid format for colony lifts. Differential colony hybridization was used to identify individual transformants containing deleted forms of the spike gene sequence.

Generation and labeling of probes. An 832-bp wild-type S1 region was PCR amplified with primers S1-1 and S1-2 (1) and subsequently cloned into pGEM-T. An 837-bp full-length probe was generated by *Eco*RI and *Bam*HI restriction digestion of the S1 wild-type-containing miniprep DNA. The resulting 837-bp fragment was purified by electrophoresis on a 1% agarose gel and eluted from the excised gel slice by centrifugation through glass wool. The gel-purified DNA was concentrated and quantitated on a 1% agarose gel, and 10 ng of it was then labeled.

The 63-bp core probe was generated by PCR amplification of wild-type S1 plasmid DNA with primers S1-5 (5′-CCATTTCGCCTCGGCAC-3′) (nt 1548 to 1546) and S1-6 (5′-TTGGGTTTACAAGTGCACTC-3′) (nt 1591 to 1610) under the PCR conditions described above. The 63-bp product was isolated by electrophoresis on a 5% nondenaturing polyacrylamide gel. The DNA was eluted from the excised gel slice in 300 μl of gel extraction buffer (1× TE, 0.4 M NaCl, 0.1% sodium dodecyl sulfate [SDS], 5 mM $MgCl_2$) by gentle mixing on a rotator for 1 h. The gel-purified DNA was concentrated by ethanol precipitation and quantitated on a 5% polyacrylamide gel. Approximately 10 ng of DNA was ligated in the presence of 1 U of T4 DNA ligase overnight at 14°C to join the 63-bp DNA into concatamers and subsequently labeled.

A 10-ng portion of either 837- or 63-bp concatameric DNA was boiled in a total volume of 38 μl for 5 min and quickly cooled on ice to generate single-stranded DNA. Denatured DNA fragments were random-primer labeled in a total volume of 50 μl by the addition of 10 μl of 5× labeling buffer, which consists of 20 μl of solution A (1.2 M Tris-HCl [pH 8.0], 0.12 M $MgCl_2$, 0.25 M β-mercaptoethanol, 0.5 mM dATP, 0.5 mM dGTP, 0.5 mM dTTP), 50 μl of solution B (2 M HEPES), and 30 μl of solution C [20 optical density units of random hexamers per ml in 3 mM Tris-HCl (pH 8.0) and 0.2 mM EDTA]; 1 μg of bovine serum albumin; 10 to 50 μCi of [α-^{32}P]dCTP (3,000 Ci/mmol [Amersham, Arlington Heights, Ill.]); and 5 U of Klenow DNA polymerase (Promega Corp., Madison, Wis.) for 1 to 2 h at room temperature. The probes were purified away from unincorporated nucleotides by elution from a G-50 Sepharose tuberculin syringe column in 200 μl of TE (Tris-EDTA [pH 8.0]). The probes were denatured in the presence of 1 mg of salmon sperm DNA by boiling for 4 min and quickly cooling on ice, and the hybridization solution was added. The probes were used at a final concentration of greater than 10^6 cpm/ml.

Differential colony hybridization. Approximately 100 colonies per transformation were picked onto a grid format with control colonies of vector alone and vector plus full-length S1 insert. Colony lifts were performed as described by Sambrook et al. (45) with 0.2-μm nitrocellulose filters (Schleicher & Schuell, Keene, N.H.). The filters were dried for 30 min at room temperature and then baked for 2 h in a vacuum oven at 80°C. They were soaked in 2× SSC (1× SSC is 0.15 M NaCl plus 0.015 M sodium citrate) for 2 min prior to prehybridization for at least 2 h at 65°C in buffer consisting of 1% SDS, 0.5 M NaCl, 10% dextran sulfate, and 100 μg of denatured salmon sperm DNA per ml. The filters were then incubated overnight at 65°C with either the full-length 837-bp probe or the core 63-bp probe (10 ng, 10^6 cpm/ml) (see Fig. 1). After hybridization, the blots were washed for 5 min at room temperature in buffer containing 2× SSC and subsequently washed in 2× SSC–0.1% SDS at 65°C for 20 min. The blots were exposed to X-ray film at −80°C for 2 to 12 h. Colonies which hybridized to the full-length 837-bp probe but not the core probe were selected for sequence analysis.

Sequencing. Plasmid DNA was isolated from selected transformants by using the Wizard Minipreps DNA purification system (Promega) and sequenced by the Sanger dideoxy chain termination method (46) with Sequenase Enzyme 2.0 (Sequenase DNA sequencing kit, version 2.0; U.S. Biochemicals) and S1 region primers (S1-2 and S1-3) (1), which flank the previously identified deletions. Thus, the majority of the clones were sequenced from nt 1450 to 1795. In cases where S1 deletions were large and extended beyond these regions, reverse and −40 primers as well as primer S1-1 (1) were used to sequence across the deletion. The reaction products were analyzed on 5% Hydrolink (J. T. Baker) gels containing 7 M urea in TBE.

RESULTS

Detection of MHV S1 RNA deletion variants. As a first step toward understanding the role of SDVs in the pathogenesis of persistent MHV infection, we established a system to detect and characterize SDVs from a population of persisting viral RNAs. This system involves amplifying an 848-bp fragment encompassing the MHV S1 hypervariable region from total RNA isolated from the brains or spinal cords of infected mice sacrificed at 4, 42, or 100 days p.i.; cloning the amplified products; and identifying deletion variants by differential colony hybridization with a probe to the entire S1 domain (837 bp) and a core probe (63 bp) which represents a domain which is consistently deleted in documented MHV variants (Fig. 1). This system allowed us to detect and characterize individual SDVs from a population of persisting viral RNAs.

We first examined the prevalence of SDVs during the acute stage of infection and within the input virus population. To determine if SDVs are detected in the acute stage of infection, we isolated RNA from the brains and spinal cords of mice at 4 days p.i. and subjected it to RT-PCR amplification, cloning, and differential hybridization (as described above). As shown in Fig. 2, the S1 domain is detected by RT-PCR analysis in both the brains and spinal cords of all 10 MHV-infected mice. Using differential colony hybridization to evaluate approximately 70 cloned isolates per mouse CNS site, we determined that 4 of the 10 acutely infected mice harbored low frequencies (1 to 3%) of SDVs (Tables 1 and 2). To determine if SDVs were present in the input virus inoculum, MHV genomic RNA was isolated and subjected to RT-PCR amplification of the S1 domain, as described in Materials and Methods. The S1 PCR products were cloned, and 849 clonal isolates were examined by differential hybridization as described above. We identified one deletion isolate, indicating that an SDV is detectable, albeit at a low frequency (1 of 849), within the input virus population (Tables 1 and 2). These results indicate that the

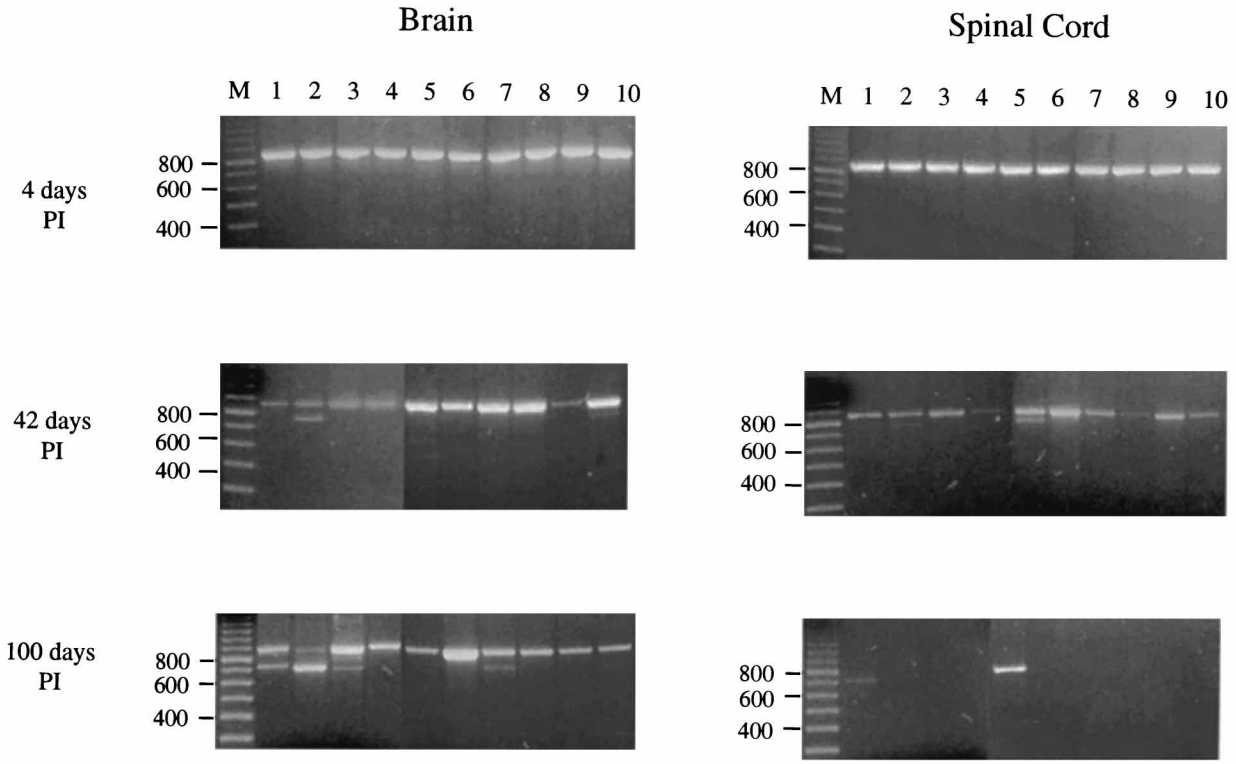

FIG. 2. Persistence and evolution of MHV-JHM 2.2-V-1 RNA in the brains and spinal cords of C57/BL6 mice. Brain and spinal cord RNA was isolated from 10 mice each on days 4, 42, and 100 p.i. and subjected to RT-PCR amplification with spike-specific primers (S1-1 and S1-2). Numbers 1 through 10 represent individual mice whose brains and spinal cords were analyzed. Individual samples were later designated by the day of sacrifice and mouse number (example 42-1), and "B" or "C" was added to indicate the origin of the RNA (brain or spinal cord) of that mouse. PCR products were analyzed by electrophoresis on a 1.5% agarose gel and visualized by ethidium bromide staining.

majority of the S1 RNAs are in fact full length both in the input virus and during the acute phase of infection. Indeed, our method of amplification and cloning may enhance our ability to detect deletion variants, since smaller PCR products may be amplified and cloned at a slightly higher efficiency than the full-length sequence. Overall, these results indicate that SDVs are detectable at a low level both in the input virus and in some mice in the acute stage of infection, before the development of a specific immune response to which escape mutants may be selected.

To determine if SDVs are detected during persistent infection, RNA isolated from the brains and spinal cords of mice sacrificed on days 42 and 100 p.i. was subjected to the same analysis. At 42 days p.i., a 848-bp S1 product was detected in both the brains and spinal cords of all 10 mice. However, additional, smaller PCR products were detected in at least five mice (Fig. 2). Cloning of the PCR products followed by differential colony hybridization showed that 7 of the 10 mice harbored SDVs (Tables 1 and 2). The SDVs represented 4 to 44% of the total S1 products from these mice. Interestingly, 3 of the 10 mice had undetectable levels of SDVs but were clearly persistently infected with MHV. Overall, these results indicate that SDVs are common but are not required for MHV persistence.

Similar results were seen in the mice sacrificed at 100 days p.i. RT-PCR amplification of MHV S1 RNA isolated from brains shows that all 10 mice were persistently infected with MHV (Fig. 2). In addition to the wild-type product of 848 bp, we identified putative deletion variant PCR products in 4 of the 10 mice. Differential hybridization of isolated clones again verified that SDVs were detected in 4 of 10 persistently infected mice (Tables 1 and 2). In contrast to the day 100 brain RNA samples, MHV S1 sequences were visualized from only 2 of 10 spinal cord RNA samples, suggesting that MHV RNA was absent or present at only very low levels in the spinal cord in the majority of mice. The integrity of all the spinal cord RNA samples was verified by amplification with primers specific to β_2-microglobulin (data not shown). Interestingly, of the two mice in which S1 RNA is detected in the spinal cord, one harbored exclusively wild-type S1 (mouse 100-5) and the other harbored exclusively SDVs (mouse 100-1) (Table 1). These results are consistent with our earlier observation that SDVs, while not required for persistent infection, may predominate in some mice during the chronic phase of disease.

Correlation of SDVs with neurological impairment. To determine if there was an association between clinical signs of demyelination and the presence of SDVs, we evaluated all mice for clinical signs of neurological disease throughout acute and persistent stages of infection. Mice were graded on a scale of 0 to 4 (0 indicating no abnormality, 1 indicating minimal gait abnormality, 2 indicating moderate paraparesis, 3 indicating severe paraparesis, and 4 indicating parapalegia). The majority of infected mice exhibited transient hind-limb paralysis (grade 3 or 4) by day 14 p.i., as expected (Table 1) and subsequently recovered. However, 5 of the 20 persistently infected mice exhibited severe and chronic neurological impairment (clinical score 4 on both days 14 and 24 [Tables 1 and 2]). These mice also harbored the highest frequencies of SDVs in their spinal cords (Fig. 3). In contrast, SDVs were less prevalent in mice with less severe signs of neurological disease (scores 1 to 3 on

TABLE 1. Detection of viral quasispecies during persistent MHV-JHM infection

Mouse and day p.i. sacrificed[a]	Clinical score[b] on p.i. day:					Brain		Spinal cord	
	4	14	24	42	100	No. of clones deleted/ no. of clones analyzed	% SDV clones	No. of clones deleted/ no. of clones analyzed	% SDV clones
Day 4									
4-1	0					2/71	3	2/71	3
4-2	0					0/71	0	0/73	0
4-3	0					0/76	0	0/73	0
4-4	0					0/80	0	1/78	1
4-6	0					0/82	0	0/82	0
4-8	0					0/82	0	0/70	0
4-9	0					2/76	3	0/79	0
4-10	0					0/78	0	0/78	0
4-7	1					0/85	0	0/72	0
4-5	1					1/76	1	0/83	0
Day 42									
42-9		3	2	1		0/73	0	0/114	0
42-8		4	2	1		0/94	0	3/74	4
42-7		3	3	2		0/70	0	3/79	4
42-4		ND	3	2		0/74	0	0/96	0
42-3		ND	3	2		0/77	0	0/75	0
42-6		4	3	2		9/89	10	0/75	0
42-10		4	3	3		6/118	5	0/72	0
42-1[c]		ND	4	2		0/71	0	5/79	11
42-5[c]		4	4	2		0/92	0	9/77	12
42-2[c]		ND	4	4		23/52	44	17/91	19
Day 100									
100-9[d]		0	1		1	0/83	0	—[e]	—
100-8		4	3		0	0/86	0	—	—
100-6		3	2		1	0/166	0	—	—
100-7		3	1		2	13/166	8	0/2	0
100-4		3	3		1	0/85	0	—	—
100-2		3	3		2	80/82	98	—	—
100-10		4	3		2	0/75	0	—	—
100-5		3	3		2	0/94	0	0/77	0
100-3[c]		4	4		3	9/83	11	—	—
100-1[c]		4	4		3	15/66	23	19/19	100

[a] Individual samples were designated by day of sacrifice and mouse number (for example, 42-1 indicates mouse number 1 sacrificed on day 42).
[b] Clinical scores: 0, normal mouse; 1, minimal gait abnormality; 2, moderate paraparesis; 3, severe paraparesis; 4, parapalegia; ND, not determined.
[c] Mice with severe and prolonged neurological disease.
[d] Detection of viral RNA in the brain indicates that this mouse was infected; however, no significant clinical signs of MHV pathogenesis were observed.
[e] —, viral RNA was not detected by RT-PCR.

day 24). Indeed, we found a statistically significant difference ($P = 0.0025$; Mann-Whitney U test) in the percentage of SDVs in the spinal cords of mice with clinical scores of 4 versus mice with clinical scores of 1 to 3 (Fig. 3). In addition, we found an overall modest but positive correlation between the clinical scores (1 to 4) of mice and the percentage of SDVs in the spinal cord and brain (Fig. 3 [Pearson correlation coefficient; $P = 0.045$ for spinal cord, $P = 0.051$ for brain]). These results suggest that the prevalence of SDVs during persistent infection is associated with more severe clinical manifestations of demyelination.

TABLE 2. Summary of analysis of SDVs identified from the brains and spinal cords of mice

Time p.i.	No. deleted/total no. of clones analyzed	No. of mice with deleted forms	% SDV clones[a]
Input virus	1/849	–[b]	0.1
Day 4	8/1,536	4/10	1–3
Day 42	75/1,642	7/10	4–44
Day 100	136/1,084	4/10	8–100

[a] Range of percent SDVs in the CNS of mice with at least one deletion.
[b] RNA was isolated from an uninfected mouse brain that was mixed with 5×10^6 PFU of MHV-JHM 2.2-V-1.

Characterization of MHV SDVs. To characterize the population of MHV deletion isolates, we sequenced 106 individual SDV clones. Of these, 58 may represent unique species distinguishable by deletions and flanking point mutations (Table 3). Twenty-three distinct patterns of SDVs were identified and are displayed according to increasing size of the deletion (Fig. 4). We also categorized the SDVs according to the time p.i. during which they were identified and the site from which they were isolated (e.g., 42B indicates brain RNA obtained on day 42 p.i.).

Several important points can be derived from this data. First, SDVs appear to arise during viral replication in the CNS. This is supported by the fact that we detected 13 isolates with deletions smaller than the single SDV identified in the input virus. These results indicate that the input SDV we detected was probably not the "founder" virus for all subsequent SDVs in the CNS. In addition, we found that the majority of SDVs were unique to an individual mouse (Fig. 4). These results

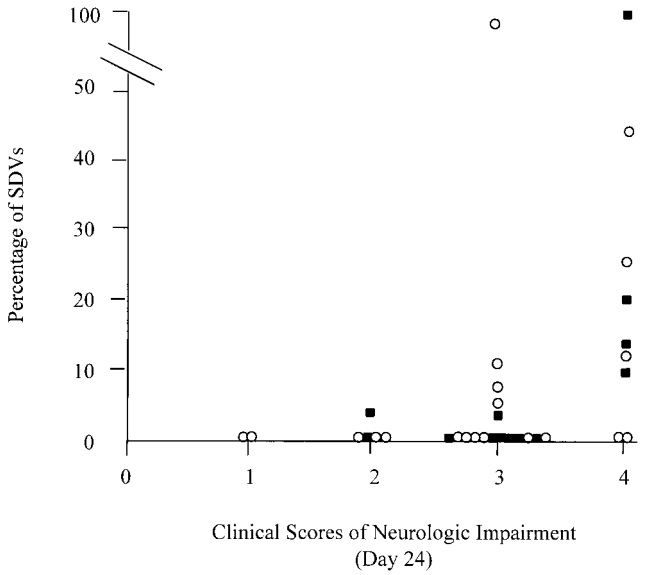

FIG. 3. Correlation of the frequency of detectable SDVs with neurological impairment. Mice sacrificed on days 42 and 100 were examined for clinical signs of hind-limb paralysis. All mice were examined at the same time point (day 24), after subacute disease commonly resolves, to identify mice that were developing prolonged or unusually severe paralysis. Clinical score: 0, normal mouse; 1, minimal gait abnormality; 2, moderate paraparesis; 3, severe paraparesis; 4, parapalegia. Differential colony hybridization was used to detect deletion variants from the brains (open circles) and spinal cord (solid squares) of mice.

suggest that the generation and evolution of SDVs is a random event within each mouse. Furthermore, within some individual mice, we detected SDVs in the brain which were distinct from those in the spinal cord (e.g., mice 42-2 and 100-1 [Table 3]). This de novo generation of MHV SDVs is consistent with the stochastic process of generating viral deletion variants, bottlenecks, and the expansion of quasispecies that has been described for other viral systems (12, 13, 23, 39).

Second, SDVs probably continue to arise throughout persistent infection. We detected a wide range of SDVs at each time p.i. For example, on day 42 p.i., SDVs ranging from 84 to 479 bp were detected. On day 100, we detected nine different SDVs ranging from 84 to 179 bp. We also detected multiple SDVs from a single site (Table 3). About half of the SDVs (52%) were in frame (Fig. 4) and thus have the potential to encode a functional S1 region of the spike glycoprotein. However, 11 of 23 SDVs detected during persistent infection were out of frame, suggesting either that these "defective" SDVs are replicated and maintained during persistent infection or that such defective RNAs are generated throughout persistent infection. Ongoing evolution of the MHV SDVs is further supported by the detection of double-deletion variants. Indeed, SDV 9 (deletion 1524 to 1625) may serve as the parent for the double-deletion variants 10 (deletions 1524 to 1625 and 1648 to 1654) and 20 (deletions 1524 to 1625 and 1425 to 1506). Both single and double SDVs were detected in the spinal cord RNA of mouse 42-2 and mouse 100-1 (Table 3). Overall, these results are consistent with continued replication and evolution of SDVs throughout persistent infection.

To determine if a particular sequence is frequently involved in recombination events, we graphed the nucleotide position of the endpoints of the SDVs identified from the 30 mice and plotted the frequency of each in independent deletion events (Fig. 5). Independent deletion events were defined by two criteria: (i) they are identified within an individual mouse or mouse CNS site, and (ii) they possess independent crossover sites. Because of the possible bias of PCR amplification and introduction of point mutations, the plotted frequency does not reflect the abundance of clones with the same deletion endpoints within an individual mouse, regardless of point mutations. We found that the SDVs generated in the mice sacrificed on days 4, 42 and 100 all cluster in a hypervariable region of S1 around nt 1500 to 1650. The nonrandom clustering of SDVs may occur as a consequence of the RNA secondary structure in the S1 domain.

We also noted that positions 1524 and 1625 are the most frequent sites involved in recombination events and that, over time, the distribution of the deletion events expands over the hypervariable region. This finding is in contrast to the clustering and eventual loss of recombinants that were generated during coinfection of MHV-A59 and MHV-JHM and passage in DBT cells (2a). This indicates that the selective pressures in the CNS are quite distinct from that of in vitro DBT culture conditions and may favor the "fitness" of different SDVs (12, 14, 23).

Detection of MHV S1 quasispecies in mice with prolonged neurological impairment. As described above, we noted that SDVs were most prevalent in mice which exhibited the most severe and prolonged clinical signs of demyelination throughout persistent infection (mice 42-1, 42-5, 42-2, 100-1, and 100-3). These severely impaired mice harbored multiple SDVs with flanking point mutations (Table 3). Two of the five mice also harbored double SDVs. These mice were striking because of the prevalence of in-frame SDVs detected in the spinal cord RNA (ranging from 11 to 100% of the S1 isolates). These results are consistent with the earlier observations of Morris et al. (40) suggesting that infectious deletion variants with altered tropism or demyelinating potential may be responsible for the more severe pathogenesis observed in some mice.

DISCUSSION

In this study, we examined the population of coronavirus spike deletion variants (SDVs) in the CNS of persistently infected mice. The approach we used was to rescue viral RNA from the CNS by RT-PCR, clone the amplified products, and detect SDVs by differential hybridization. Our initial studies were directed to the S1 hypervariable region, since previous investigators have shown that this region is subject to recombination and deletion (Fig. 1). We found that the majority of persistently infected mice harbored a mixture or quasispecies of full-length and deleted forms of the MHV S1 region. We detected both in-frame and out-of-frame SDVs and a number of double-deletion variants, suggesting that SDVs may be generated and continue to evolve throughout persistent infection.

In the acute phase of infection (day 4), we detected SDVs in 4 of 10 mice. At this stage, SDVs represented no more than 3% of the viral RNA population. Thus, low percentages of SDVs, undetectable by agarose gel electrophoresis, could be detected by differential colony hybridization. These SDVs were probably generated during viral replication in the CNS since they are distinct from the SDV we identified in the input virus. The detection of SDVs on day 4 suggests that deletions are generated at a low frequency even before specific humoral and cellular immune responses can select viral SDVs from the viral population; i.e., SDVs generated acutely may be favored by pressure from the innate immune response or by intrinsic requirements of replication in CNS cells. In the chronic phase of infection (days 42 and 100), we detected SDVs in 11 of 20 mice. These results indicate that SDVs are common but are not required for persistent infection. In mice in which SDVs

TABLE 3. Characterization of mutations and deletions detected in the S1 region of the spike during persistent MHV-JHM infection

Mouse[a]	Clone(s)	Deletion	Open reading frame	Point mutation	Codon change	Amino acid change
Input	1	1473–1625	+			
4-1(B)	1, 2	1524–1625	+	1634 G→A	CGC→CAC	R→H
				1654 A→G	ATT→GTT	I→V
4-1(C)	1, 2	1524–1625	+	1634 G→A	CGC→CAC	R→H
				1654 A→G	ATT→GTT	I→V
4-4(C)	1	1499–1672	+			
4-5(B)	1	1526–1625	−			
4-9(B)	1, 2	1524–1625	+	1634 G→A	CGC→CAC	R→H
				1654 A→G	ATT→GTT	I→V
42-1(C)[b]	1	1524–1616	+	1636 T→C	TGT→CGT	C→R
				1674 T→C	CAT→CAC	H→H
				1746 T→C	AAT→AAC	N→N
	2, 3	1524–1616	+			
	4	1530–1616	+			
	5	1411–1646	−			
42-2(B)[b]	1	1524–1625	+	1744 A→T	AAT→TAT	N→Y
	2	1524–1625	+	1718 A→G	GAT→GGT	D→G
	3–10	1524–1625	+			
42-2(C)[b]	1	1524–1625	+	1829 T→C	ATT→ACT	I→T
	2–8	1524–1625	+			
	9[c]	1524–1625	−	1752 T→C	CTT→CCT	L→P
		1648–1654				
	10[c]	1425–1506	−			
		1524–1625				
42-5(C)[b]	1	1533–1616	+	1691 T→A	GTT→GAT	V→N
				1763 G→C	TGG→TCG	W→S
	2	1533–1616	+	1521 T→C	CAT→CAC	H→H
	3	1533–1616	+	1654 A→G	ATT→GTT	I→V
	4	1533–1616	+	1634 G→A	CGC→CAC	R→H
				1501 T→G	TGC→GGC	C→G
	5	1533–1616	+	1485 A→G	AAA→AAG	K→K
	6–8	1533–1616	+			
	9	1499–1813	+	1891 G→T	GTT→TTT	V→F
				1422 G→C	GTG→GTC	V→V
42-6(B)[b]	1–4	1473–1625	+			
	5–6	1524–1616	+			
	7–8	1524–1625	+	1654 A→G	ATT→GTT	I→V
	9	1524–1625	+	1654 A→G	ATT→GTT	I→V
				1634 G→A	CGC→CAC	R→H
42-7(C)[b]	1[c]	1520–1627	−			
		1513–1514				
	2	1526–1616	−	1456 A→G	ATA→GTA	I→V
	3	1528–1625	−	1797 C→T	CCA→TCA	P→S
42-8(C)	1	1305–1783	−			
	2	1305–1783	−	1825 G→A	TGG→TAG	W→Term
	3	1305–1783	−	1864 T→C	ATT→ACT	I→T
42-10(B)	1–4	1532–1618	+			
	5	1532–1618	+	1682 G→A	GGT→GAT	G→D
	6	1532–1618	+	1749 T→C	GAT→GAC	D→D
100-1(B)	1	1497–1645	−	1445 C→T	GCA→GTA	A→V
	2	1497–1645	−	1677 T→G	TGA→GGA	Term→G
				1702 A→G	TAA→TGA	Term→Term
	3	1497–1645	−	1799 A→G	CCA→CCG	P→P

Continued on following page

TABLE 3—*Continued*

Mouse[a]	Clone(s)	Deletion	Open reading frame	Point mutation	Codon change	Amino acid change
	4	1497–1645	−	1816 T→C	ATT→ACT	I→T
	5	1497–1645	−	1861 C→A	ACA→ATA	T→I
	6–10	1497–1645	−			
100-1(C)[b]	1	1473–1625	+	1677 T→C	TGT→TGC	C→C
	2–5	1473–1625	+			
	6[c]	1473–1625 1737–1763	+	1730 G→A	GGC→GAC	G→N
	7–9[c]	1473–1625 1735–1761	+			
	10	1533–1616	+	1478 A→G 1718 A→G	CAG→CGG GAT→GGT	Q→R D→G
100-2(B)	1	1499–1654	+	1494 T→C	TCT→TCC	S→S
	2	1499–1654	+	1695 A→T	TTA→TTT	L→F
	3	1499–1654	+	1720 C→T	TCC→TTC	S→F
	4	1499–1654	−	1763 G→A	TGG→TAG	W→Term
	5–9	1499–1654	+			
100-3(B)[b]	1	1495–1673	−	1690 G→C	TGT→TCT	C→S
	2–4	1495–1673	−			
	5–10	1532–1620	−			
100-7(B)	1, 2	1524–1646	+	1490 T→A	ATG→AAG	M→K
	3	1524–1646	+	1728 G→A	AAG→AAA	K→K
	4–10	1524–1646	+			

[a] Individual samples were designated by day of sacrifice, mouse number, site of RNA isolation [brain (B), cord (C)], and clone number, for example, 42-1(C)4 indicates mouse 1 sacrificed at day 42 p.i., spinal cord sample, clone 4.
[b] Mice with more than one type of deletion.
[c] Clone contains a double deletion.

were detected, we found an expansion in the diversity of the SDVs (compared with the acute phase), in terms of both the percentage of the population (4 to 100% of the amplified RNA) and the complexity of the SDVs, as seen in double SDVs. These results are consistent with continued evolution of the viral RNA during persistent infection.

To assess the biological importance of SDVs in the pathogenesis of demyelinating disease, we monitored the mice for clinical signs of neurological disease. Following MHV infection, most mice experienced transient hind-limb paralysis on day 14 p.i. The majority of mice recover, exhibiting less severe clinical signs of neurological impairment. Interestingly, we found the most diverse collection of SDVs in the mice with the most severe clinical disease and most impaired recovery (as defined by clinical score of 4 on both days 14 and 24). However, the reason for this severe disease is currently unclear. The presence of SDVs may reflect an initial high level of viral replication in the CNS and therefore more opportunity to generate SDVs, but the SDVs themselves may not be pathogenic. Alternatively, SDVs may be propagated by selective advantage, such as altered tropism, or reduced fusogenicity and cytopathic effects. A subset of SDVs may be responsible for the chronic demyelination that we and other investigators have reported (40, 54).

Our study suggests that critical determinants of pathogenesis in an individual mouse may be the particular expansion and selection of viral RNA quasispecies which occur within that mouse, especially during the early stages of infection (13, 14, 23). Such stochastic processes may contribute to the diversity of disease outcomes observed when inbred mice are challenged with aliquots of the same viral pool. In fact, several prior studies have suggested that subtle variations in input MHV may have a crucial influence on disease course. For example, Wege et al. (54) showed that inoculation of uncloned MHV-JHM induced a spectrum of acute and subacute diseases whereas inoculation of plaque-purified MHV-JHM (large or small plaque) predominantly caused a fatal, acute disease. Also, Morris et al. (40) reported that inoculation of the spike deletion isolate AT11f into rats caused a range of pathogenesis as monitored by the pattern of neurological lesions. Taken together, these studies and our present results suggest that minor differences in input virus or virus replicating shortly after inoculation of an individual animal may be progressively amplified and result in major differences in the ultimate disease outcome. Our demonstration that SDVs are infrequent in in vitro viral stocks but often are the predominant viral RNA species in mice with severe and chronic disease is consistent with this hypothesis and suggests that SDVs, once generated in vivo, may be subject to strong positive selection. Future studies will address these issues in more detail by inoculating mice with defined mixtures of viruses with distinct S genotypes and then analyzing subsequent disease course and progeny S genotypes.

We note that these SDVs deleted a recently identified T-cell epitope (nt 1528 to 1554) (3, 6, 43a) which overlaps with the core probe (nt 1548 to 1610) used to detect SDVs by differential colony hybridization (Fig. 4). Interestingly, the SDVs exist as a mixed population with wild-type S1 sequences, suggesting that loss of the T-cell epitope is not required for persistent infection. The persisting mixed population or quasispecies may induce "antigenic oscillations" (4, 9, 29, 30, 41) in which subdominant epitopes are recognized by T cells. Antigenic oscillation has been proposed as a mechanism contrib-

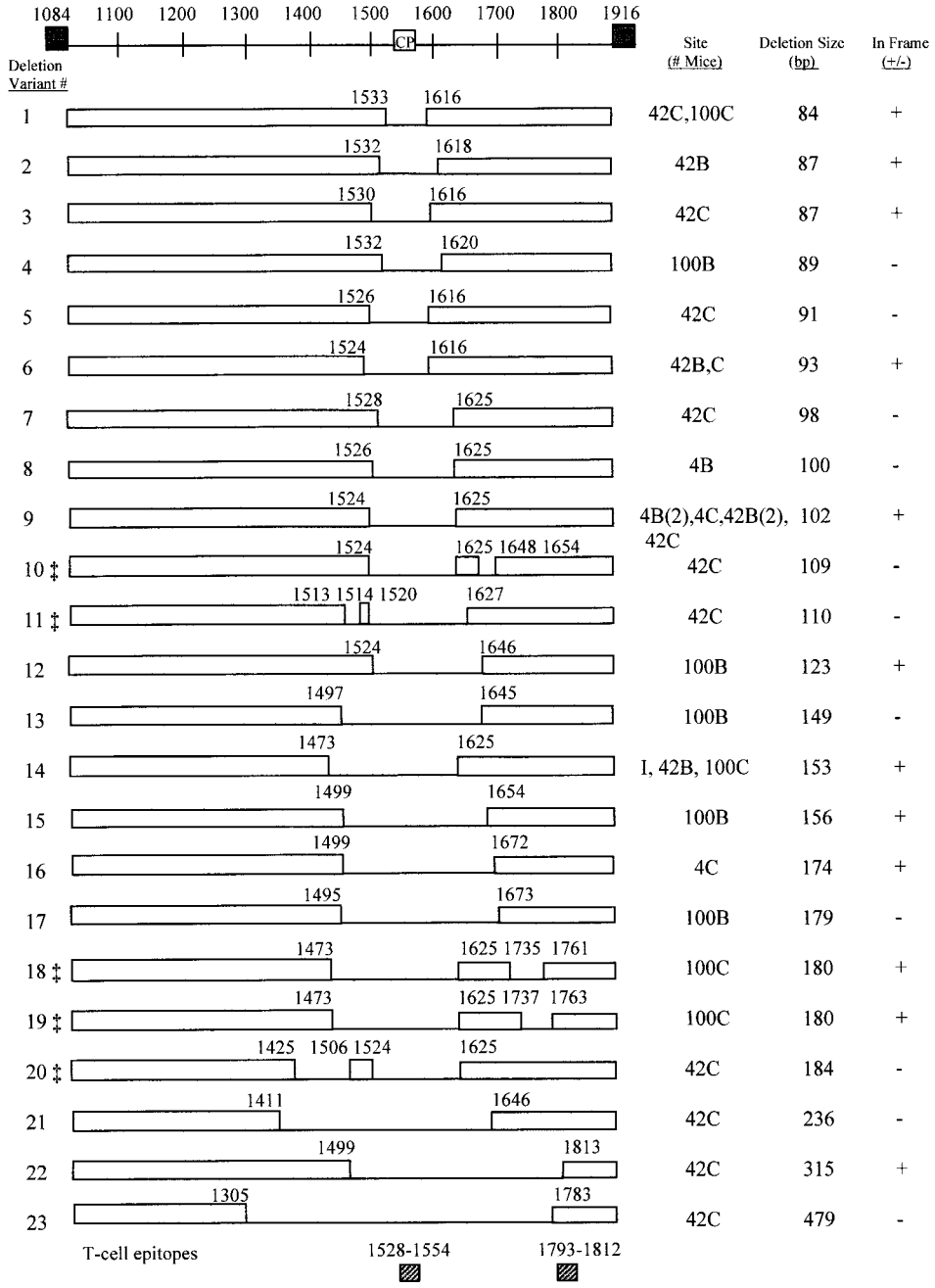

FIG. 4. Schematic representation of deletions identified in the S1 region of the spike gene (SDVs). The S1 RT-PCR products of 30 mice were analyzed by differential colony hybridization to identify individual clones with deletions. A total of 23 independent SDV patterns were identified by sequencing isolated clones and are designated 1 to 23 by increasing size of deletion. SDVs were designated according to the time p.i. when they were identified. I, input virus; 4B, day 4 brain; 4C, day 4 spinal cord; 42B, day 42 brain; 42C, day 42 spinal cord; 100B, day 100 brain; 100C, day 100 spinal cord. SDVs were identified in only one mouse during the indicated time p.i. unless otherwise indicated. CP, core probe; ‡, double-deletion variants. T-cell epitopes are as identified by Castro and Perlman (6).

uting to the inability of the immune system to effectively clear viral infections (42).

The mechanism proposed to be responsible for generating MHV SDVs is copy choice RNA recombination (27, 32, 38). Experimental evidence for copy choice RNA recombination suggests that the recombination of RNA viruses occurs most frequently during negative-strand synthesis (5, 26, 28, 35). According to this model, SDVs may be generated when a nascent RNA dissociates from the positive-strand template and rebinds to alternative sites on the template RNA. The rejoining of the nascent RNA may occur at regions of homology at the site of dissociation (homologous recombination), at alternative regions of homology (aberrant-homologous recombination), or at distinct, nonhomologous sites (nonhomologous recombination). Aberrant-homologous recombination has been proposed as a mechanism for generating deleted RNA genomes for a number of RNA viruses including MHV (2) and flock house virus (35). Aberrant-homologous recombination appears to require only short stretches of homologous sequence (3 to 7 nt). In our study, we found that seven SDVs (SDV 6, 9, 11, 13, 15,

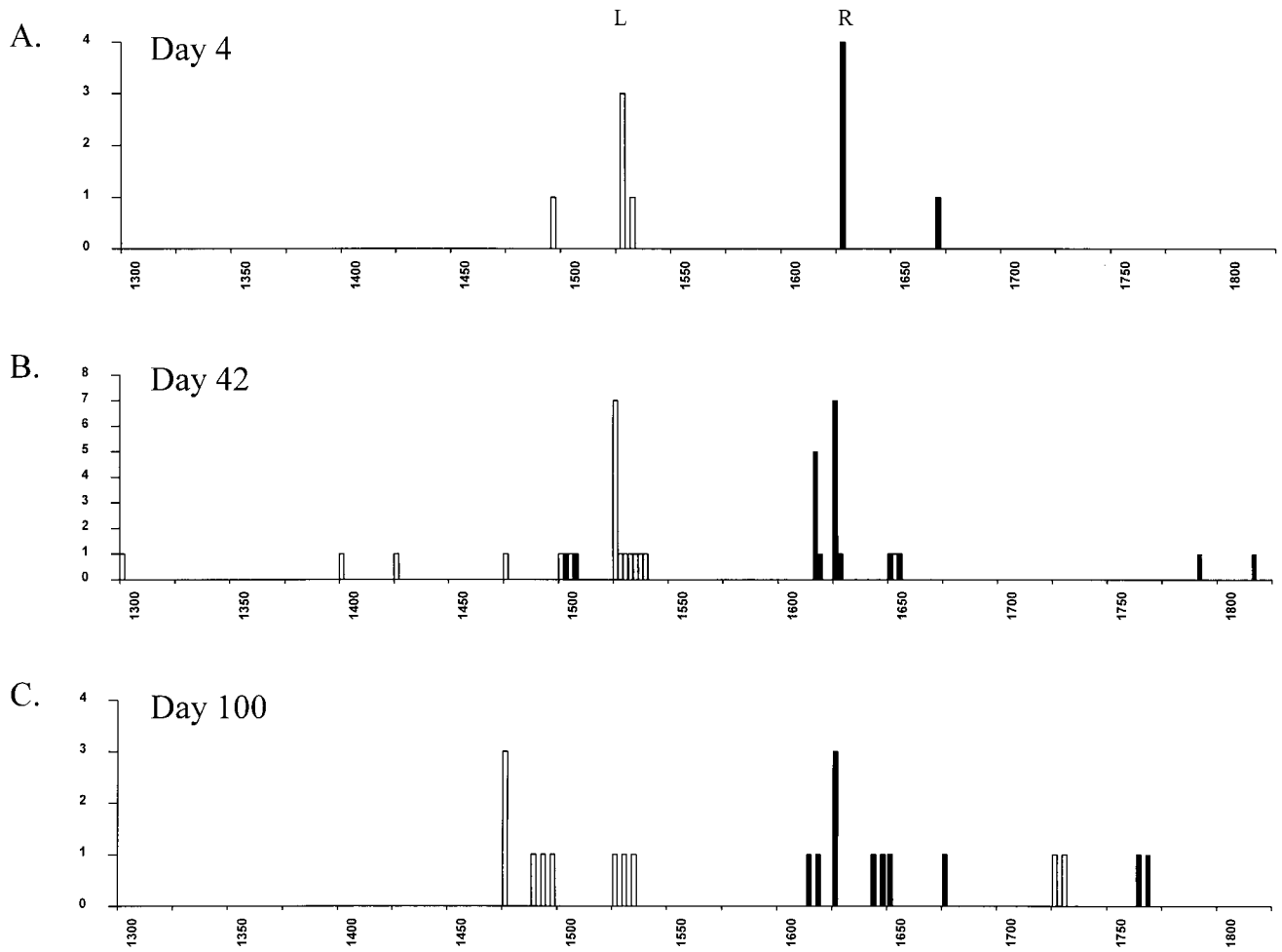

FIG. 5. Frequency distribution of crossover sites of SDVs identified from 30 mice sacrificed on day 4 (A), day 42 (B), and day 100 (C) p.i. The nucleotide positions (*x* axis) of the endpoints of the left (open bars) and right (solid bars) sequence are indicated. The frequency (*y* axis) of endpoints in independent deletion events is shown. Independent deletion events are those arising in an individual mouse in either the brain or spinal cord. Designation of left and right crossover sites is based on copy choice RNA recombination, which may occur during either positive- or negative-strand RNA synthesis.

16, and 22) have short (3- to 4-nt) regions of homology between the putative donor and junction sites. Significantly, the majority of the MHV SDVs did not possess regions of homology at the putative crossover sites and therefore were most probably generated by nonhomologous recombination.

It is currently unclear why the S1 hypervariable region is so frequently involved in generating the SDVs. As previously proposed by Banner et al. (2), one possibility is that during RNA synthesis, an RNA secondary structure in the S1 domain causes the RNA polymerase to pause and thereby promotes the dissociation of the nascent RNA from the template. The replication complex would then be available to rejoin the template by homologous or nonhomologous RNA recombination. Alternatively, copy choice recombination may be occurring randomly throughout the MHV RNA, and only RNA species that are selected during persistent infection are propagated (2a). Indeed, both high-frequency recombination sites and selective pressures may well contribute to the ultimate population of MHV RNAs detected during persistent infection. Future studies will be directed at investigating the role of the RNA secondary structure and selective pressures in the generation of MHV SDVs and quasispecies expansion during persistent infection.

ACKNOWLEDGMENTS

We thank Youlian Liao for statistical analysis of clinical data, Joan Pooley for technical assistance, and Tom Gallagher and Jennifer Schiller for helpful discussions.

This work was supported by Public Health Service research grant AI32065 from the National Institutes of Health (to S.C.B.), National Multiple Sclerosis Society research grant RG2283-A-2 (to J.O.F.), and a Department of Veterans Affairs merit review grant (to J.O.F.).

REFERENCES

1. **Adami, C., J. Pooley, J. Glomb, E. Stecker, F. Fazal, J. O. Fleming, and S. C. Baker.** 1995. Evolution of mouse hepatitis virus (MHV) during chronic infection: quasispecies nature of the persisting MHV RNA. Virology **209:** 337–346.
2. **Banner, L. R., J. G. Keck, and M. M. C. Lai.** 1990. A clustering of RNA recombination sites adjacent to a hypervariable region of the peplomer gene of murine coronavirus. Virology **175:**548–555.

2a. **Banner, L. R., and M. M. C. Lai.** 1991. Random nature of coronavirus RNA recombination in the absence of selection pressure. Virology **185:**441–445.

3. **Bergmann, C. C., Q. Yao, M. Lin, and S. A. Stohlman.** 1996. The JHM strain of mouse hepatitis virus induces a spike protein-specific D-b-restricted cytotoxic T cell response. J. Gen. Virol. **77:**315–325.
4. **Bertoletti, A., A. Sette, F. V. Chisari, A. Penna, M. Levrero, M. De Carli, F. Fiaccadori, and C. Ferrari.** 1994. Natural variants of cytotoxic epitopes are T-cell receptor are antagonists for antiviral cytotoxic T cells. Nature **369:** 407–410.
5. **Cascone, P. J., T. F. Haydar, and A. E. Simon.** 1993. Sequences and struc-

tures required for recombination between virus-associated RNAs. Science **260:**801–805.
6. **Castro, R. F., and S. Perlman.** 1995. $CD8^+$ T-cell epitopes within the surface glycoprotein of a neurotropic coronavirus and correlation with pathogenicity. J. Virol. **69:**8127–8131.
7. **Chang, S. Y., A. Shih, and S. Kwok.** 1993. Detection of variability in natural populations of viruses by polymerase chain reaction. Methods Enzymol. **224:**428–432.
8. **Collins, A. R., R. L. Knobler, H. Powell, and M. J. Buchmeier.** 1982. Monoclonal antibodies to murine hepatitis-4 (strain JHM) define the viral glycoprotein responsible for attachment and cell fusion. Virology **119:**358–371.
9. **Couillin, I., B. Culmann-Penciolelli, E. Gomard, J. Choppin, J.-P. Levy, J.-G. Guillet, and S. Saragosti.** 1994. Impaired cytotoxic T lymphocyte recognition due to genetic variations in the main immunogenic region of the human immunodeficiency virus 1 NEF protein. J. Exp. Med. **180:**1129–1134.
10. **Dales, S., and R. Anderson.** 1995. Pathogenesis and diseases of the central nervous system caused by murine coronaviruses, p. 257–384. *In* S. G. Siddell (ed.), The Coronaviridae. Plenum Press, New York, N.Y.
11. **Dalziel, R. G., P. W. Lampert, P. J. Talbot, and M. J. Buchmeier.** 1986. Site specific alteration of murine hepatitis virus type 4 peplomer glycoprotein E2 results in reduced neurovirulence. J. Virol. **59:**463–471.
12. **Domingo, E., C. Escarmis, M. A. Martinex, E. Martinez-Salas, and M. G. Mateau.** 1992. Foot-and-mouth disease virus populations are quasispecies. Curr. Top. Microbiol. Immunol. **176:**33–47.
13. **Duarte, E. A., I. S. Novella, S. C. Weaver, E. Domingo, S. Wain-Hobson, D. K. Clarke, A. Moya, S. F. Elena, J. C. de la Torre, and J. J. Holland.** 1994. RNA virus quasispecies: significance for viral disease and epidemiology. Infect. Agents Dis. **3:**201–214.
14. **Eigen, M.** 1993. The origin of genetic information: viruses as models. Gene **135:**37–47.
15. **Fazakerley, J. K., S. E. Parker, F. Bloom, and M. J. Buchmeier.** 1992. The V5A13.1 envelope glycoprotein deletion mutant of mouse hepatitis virus type-4 is neuroattenuated by its reduced rate of spread in the central nervous system. Virology **187:**178–188.
16. **Fazakerley, J. K., and M. J. Buchmeier.** 1993. Pathogenesis of virus-induced demyelination. Adv. Virus Res. **42:**249–324.
17. **Fleming, J. O., M. D. Trousdale, F. A. K. El-Zaatari, and S. A. Stohlman.** 1986. Pathogenicity of antigenic variants of murine coronavirus JHM selected with monoclonal antibodies. J. Virol. **58:**869–875.
18. **Fleming, J. O., M. D. Trousdale, J. Bradbury, S. A. Stohlman, and L. P. Weiner.** 1987. Experimental demyelination induced by coronavirus JHM (MHV-4): molecular identification of a viral determinant of paralytic disease. Microb. Pathog. **3:**9–20.
19. **Fleming, J. O., and L. B. Pen.** 1988. Measurement of the concentration of murine IgG monoclonal antibody in hybridoma supernatants and ascites in absolute units by sensitive and reliable enzyme-linked immunosorbent assay (ELISA). J. Immunol. Methods **110:**8–11.
20. **Fleming, J. O., F. I. Wang, M. D. Trousdale, D. R. Hinton, and S. A. Stohlman.** 1993. Interaction of immune and central nervous systems: Contribution of antiviral Thy-1+ cells to demelination induced by coronavirus JHM. Reg. Immunol. **5:**37–43.
21. **Fleming, J. O., C. Adami, J. Pooley, J. Glomb, E. Stecker, F. Fazal, and S. C. Baker.** 1995. Mutations associated with viral sequences isolated from mice persistently infected with MHV-JHM. Adv. Exp. Med. Biol. **380:**591–595.
22. **Gallagher, T. M., S. E. Parker, and M. J. Buchmeier.** 1990. Neutralization-resistant variants of a neurotropic coronavirus generated by deletions within the amino-terminal half of the spike glycoprotein. J. Virol. **64:**731–741.
23. **Holland, J. J.** 1993. Replication error, quasispecies populations and extreme evolution rates of RNA viruses, p. 203–218. *In* S. S. Morse (ed.), Emerging viruses. Oxford University Press, Oxford, United Kingdom.
24. **Holmes, K. V., and M. M. C. Lai.** 1996. Coronaviridae: the viruses and their replication, p. 1075–1093. *In* B. N. Fields, D. M. Knipe, P. M. Howley, et al. (ed.), Fields virology. Lippincott-Raven Publishers, Philadelphia, Pa.
25. **Jackson, D. P., D. H. Percy, and V. L. Morris.** 1984. Characterization of murine hepatitis virus (JHM) RNA from rats with experimental encephalomyelitis. Virology **137:**297–304.
26. **Jarvis, T. C., and K. Kirkegaard.** 1992. Poliovirus RNA recombination: mechanistic studies in absence of selection. EMBO J. **11:**3135–3145.
27. **Keck, J. G., G. K. Matsushima, S. Makino, J. O. Fleming, D. M. Vannier, S. A. Stohlman, and M. M. C. Lai.** 1988. In vivo RNA-RNA recombination of coronavirus in mouse brain. J. Virol. **62:**1810–1813.
28. **Kirkegaard, K., and D. Baltimore.** 1986. The mechanism of RNA recombination in poliovirus. Cell **47:**433–443.
29. **Klenerman, P., S. Rowland-Jones, S. McAdam, J. Edwards, S. Daenke, D. Lalloo, B. Koppe, W. Rosenberg, D. Boyd, A. Edwards, P. Giangrande, R. E. Phillips, and A. J. McMichael.** 1994. Cytotoxic T-cell activity antagonized by naturally occurring HIV-1 gag variants. Nature **369:**403–407.
30. **Kodama, T., K. Mori, T. Kawahara, D. J. Ringler, and R. C. Desrosiers.** 1993. Analysis of simian immunodeficiency virus sequence variation in tissues of rhesus macaques with simian AIDS. J. Virol. **67:**6522–6534.
31. **Kyuwa, S., and S. A. Stohlman.** 1990. Pathogenesis of a neurotropic murine coronavirus, strain JHM in the central nervous system of mice. Semin. Virol. **1:**273–280.
32. **Lai, M. M. C.** 1992. RNA recombination in animal and plant viruses. Microbiol. Rev. **56:**61–79.
33. **La Monica, N., L. R. Banner, V. L. Morris, and M. M. C. Lai.** 1991. Localization of extensive deletions in the structural genes of two neurotropic variants of murine coronavirus JHM. Virology **182:**883–888.
34. **Lavi, E., D. H. Gilden, M. K. Highkin, and S. R. Weiss.** 1986. The organ tropism of mouse hepatitis virus A59 in mice is dependent on dose and route of inoculation. Lab. Anim. Sci. **36:**130–135.
35. **Li, Y., and L. A. Ball.** 1993. Nonhomologous RNA recombination during negative-strand synthesis of flock house virus RNA. J. Virol. **67:**3854–3860.
36. **Luytjes, W., L. S. Sturman, P. J. Bredenbeek, J. Charite, B. A. M. van der Zeust, M. C. Horzinek, and W. J. M. Spaan.** 1987. Primary structure of the glycoprotein E2 of coronavirus MHV-A59 and identification of the trypsin cleavage site. Virology **161:**479–487.
37. **Makino, S., F. Taguchi, M. Hayami, and K. Fujiwara.** 1983. Characterization of small plaque mutants of mouse hepatitis virus, JHM strain. Microbiol. Immunol. **27:**445–454.
38. **Makino, S., J. G. Keck, S. A. Stohlman, and M. M. C. Lai.** 1986. High-frequency RNA recombination of murine coronaviruses. J. Virol. **57:**729–737.
39. **Martell, M., J. I. Esteban, J. Quer, J. Genesca, A. Weiner, R. Esteban, J. Guardia, and J. Gomez.** 1992. Hepatitis C virus (HCV) circulates as a population of different but closely related genomes: quasispecies nature of HCV genome distribution. J. Virol. **66:**3225–3229.
40. **Morris, V. L., C. Tieszer, J. Mackinnon, and D. Percy.** 1989. Characterization of coronavirus JHM variants isolated from Wistar Furth rats with a viral-induced demyelinating disease. Virology **169:**127–136.
41. **Moskophidis, D., and R. M. Zinkernagel.** 1995. Immunobiology of cytotoxic T-cell escape mutants of lymphocytic choriomeningitis virus. J. Virol. **69:**2187–2193.
42. **Nowak, M. A., R. M. May, R. E. Phillips, S. Rowland-Jones, D. G. Lalloo, S. McAdam, P. Klenerman, B. Koppe, K. Sigmund, C. R. V. Bangham, and A. J. McMichael.** 1995. Antigenic oscillations and shifting immunodominance in HIV-1 infections. Nature **375:**606–611.
43. **Parker, S., T. M. Gallagher, and M. J. Buchmeier.** 1989. Sequence analysis reveals extensive polymorphism and evidence of deletions within the E2 glycoprotein gene of several strains of murine hepatitis virus. Virology **173:**664–673.

43a. **Pewe, L., G. F. Wu, E. M. Barnett, R. F. Castro, and S. Perlman.** 1996. Cytotoxic T cell-resistant variants are selected in a virus-induced demyelinating disease. Immunity **5:**253–262.

44. **Saiki, R. K., D. H. Gelfand, S. Stoffel, S. J. Scharf, R. Higuchi, G. T. Horn, K. B. Mullis, and H. A. Erlich.** 1988. Primer-directed enzymatic amplification of DNA with a thermostable DNA polymerase. Science **239:**487–491.
45. **Sambrook, J., E. F. Fritsch, and T. Maniatis.** 1989. Molecular cloning: a laboratory manual, 2nd ed. Cold Spring Harbor Laboratory Press, Cold Spring Harbor, N.Y.
46. **Sanger, F., S. Nicklen, and A. R. Coulson.** 1977. DNA sequencing with chain-terminating inhibitors. Proc. Natl. Acad. Sci. USA **74:**5463–5467.
47. **Schmidt, I., M. Skinner, and S. Siddell.** 1987. Nucleotide sequence of the gene encoding the surface projection glycoprotein of coronavirus MHV-JHM. J. Gen. Virol. **68:**47–56.
48. **Siddell, S. G.** 1995. The coronaviridae: an introduction, p. 1–9. *In* S. G. Siddell (ed.), The Coronaviridae. Plenum Press, New York, N.Y.
49. **Stohlman, S. A., and L. P. Weiner.** 1981. Chronic central nervous system demyelination in mice after JHM virus infection. Neurology **31:**38–44.
50. **Sturman, L. S., C. S. Ricard, and K. V. Holmes.** 1985. Proteolytic cleavage of the E2 glycoprotein of murine coronavirus: activation of cell-fusing activity of virions by trypsin and separation of two different 90K cleavage fragments. J. Virol. **56:**904–911.
51. **Taguchi, F., T. Ikeda, and H. Shida.** 1992. Molecular cloning and expression of a spike protein of neurovirulent murine coronavirus JHMV variant cl-2. J. Gen. Virol. **73:**1065–1072.
52. **Taguchi, F., H. Kubo, H. Takahashi, and H. Suzuki.** 1995. Localization of neurovirulence determinant for rats on the S1 subunit of murine coronavirus JHMV. Virology **208:**67–74.
53. **Wang, F.-I., J. O. Fleming, and M. M. C. Lai.** 1992. Sequence analysis of the spike protein gene of murine coronavirus variants: study of genetic sites affecting neuropathogenicity. Virology **186:**742–749.
54. **Wege, H., M. Koga, R. Watanabe, K. Nagashima, and V. ter Meulen.** 1983. Neurovirulence of murine coronavirus JHM temperature-sensitive mutants in rats. Infect. Immun. **39:**1316–1324.
55. **Wege, H., J. Winter, and R. Meyermann.** 1988. The peplomer protein E2 of coronavirus JHM as a determinant of neurovirulence: definition of critical epitopes by variant analysis. J. Gen. Virol. **69:**87–98.